

## Additional magnetoelectric effect in electrode-arrayed magnetoelectric composite

D. A. Pan,<sup>1,a</sup> Z. J. Zuo,<sup>1</sup> S. G. Zhang,<sup>1</sup> B. Liu,<sup>1</sup> L. J. Qiao,<sup>1</sup> and A. A. Volinsky<sup>2</sup>

<sup>1</sup>*Institute of Advanced Materials and Technology, University of Science and Technology  
Beijing, Beijing 100083, China*

<sup>2</sup>*Department of Mechanical Engineering, University of South Florida, Tampa FL 33620, USA*

(Received 4 July 2014; accepted 29 October 2014; published online 7 November 2014)

An electrode-arrayed magnetoelectric (ME) composite was proposed, in which the positive and negative electrodes of the PZT-5H plate ( $\text{Pb}(\text{Zr}_{0.52}\text{Ti}_{0.48})\text{O}_3$ ) were equally divided into a  $2 \times 5$  array, while the PZT plate remained intact. The ME voltage coefficients of these 10 sections were measured individually and in parallel/series modes. The magnetoelectric coefficient is doubled compared with un-arrayed condition, when the 10 sections are connected in parallel/series using an optimized connecting sequence derived from the charge matching rule. This scheme can also be applied to other types of layered magnetoelectric composites to obtain additional magnetoelectric effect from the original composite structure. © 2014 Author(s). All article content, except where otherwise noted, is licensed under a Creative Commons Attribution 3.0 Unported License. [<http://dx.doi.org/10.1063/1.4901564>]

Magnetoelectric materials have drawn increasing interest due to their magnetic/electric energy conversion ability.<sup>1,2</sup> Magnetoelectric materials, including single-phase compounds<sup>3–5</sup> and composites, are considered as promising candidates for multiple applications.<sup>6–11</sup> Magnetoelectric composites exhibit the advantages of large magnetoelectric effect at room temperature and great design flexibility. To constantly improve the magnetoelectric effect of the ME composites, various magnetostrictive/piezoelectric systems have been employed, including  $\text{CoFe}_2\text{O}_4/\text{Pb}(\text{Zr,Ti})\text{O}_3$ ,  $\text{Ni}/\text{Pb}(\text{Zr,Ti})/\text{Ni}$ , Terfenol-D/PVDF and Terfenol-D/epoxy- $\text{Pb}(\text{Zr,Ti})\text{O}_3$  composites.<sup>12–16</sup> From the perspective of composite structure, layered, multi-faceted, disk-ring and other hetero-structures have been developed.<sup>17–21</sup>

Arrayed structure can improve system performance and achieve multiple functions for multiple applications. It has been applied to energy harvester,<sup>22</sup> structural health monitoring device,<sup>23</sup> ultrasonic transducer,<sup>24</sup> bulk acoustic wave gravimetric chemical sensors<sup>25</sup> and other applications. Nan et al.<sup>26</sup> reported a kind of multiferroic and multifunctional composite with  $\text{Pb}(\text{Zr,Ti})\text{O}_3$  rod arrays embedded in a ferromagnetic medium of  $(\text{Tb,Dy})\text{Fe}_2/\text{epoxy}$ . The large magnetoelectric effect at high frequency was observed. However, the dice-and-fill method used to prepare the rod arrays was relatively complex. Dong, Zhai et al. applied the arrayed concept to the push-pull mode magnetostrictive/piezoelectric laminate composite.<sup>27,28</sup> They reported a composite consisting of a 1D phase connected piezoelectric PZT-fiber layer laminated between two two-dimensional phases connected high-permeability magnetostrictive FeBSiC alloy foils with interdigitated (ID) electrodes placed between them. This configuration not only optimizes stress transfer, but also enhances the dielectric capacitance of the laminate. High ME effect of 22 V/cm Oe at 1 Hz had been found, which represented the near-ideal ME coupling. Xing et al.<sup>29</sup> analyzed the noise cancellation ability of the push-pull mode and other ME configurations. Design principle of the ME sensors with the in-built capabilities to cancel environmental noise had been presented, quite useful for the enhancement of the ME effect and ME applications. In this letter, an electrode-arrayed magnetoelectric composite is described. The ME voltage coefficients of the individual sections were investigated, and when connected in parallel or in series.

<sup>a</sup>Corresponding author: Tel: +8610-82376835, Fax: +8610-62333375; E-mail address: [pandean@mater.ustb.edu.cn](mailto:pandean@mater.ustb.edu.cn)



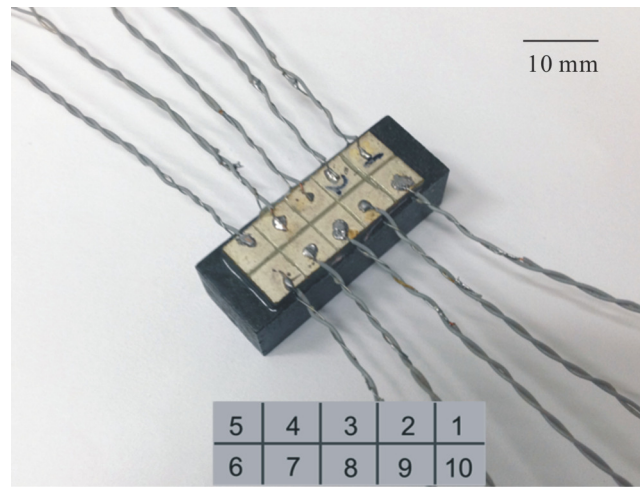
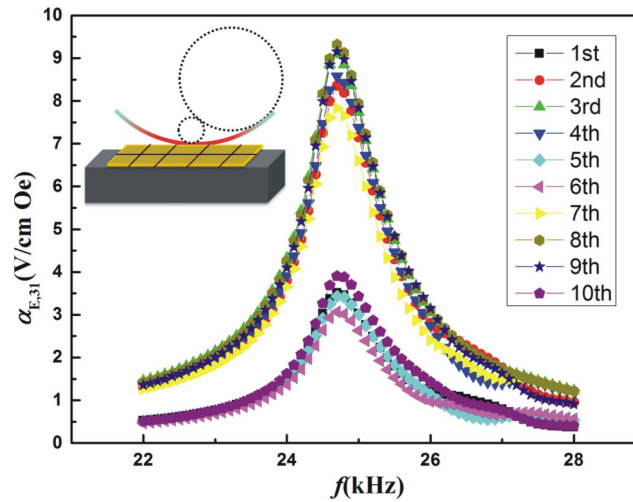


FIG. 1. The electrode-arrayed magnetolectric composite.

The electrode-arrayed magnetolectric composite is shown in Fig. 1. A commercial PZT-5H( $\text{Pb}(\text{Zr,Ti})\text{O}_3$ ) ceramic plate with  $25 \times 10 \times 1 \text{ mm}^3$  dimensions was polarized along the thickness direction. The positive and negative electrodes of the PZT plate were equally divided into a  $2 \times 5$  array, while the PZT plate remained intact. The 10 sections were electrically isolated from each other. The electrical wires were soldered to every electrode section. This arrayed PZT plate was then glued to a bonded Terfenol-D composite with  $33 \times 10 \times 10 \text{ mm}^3$  dimensions to form the electrode-arrayed magnetolectric composite. The electrode of PZT plate was also electrically isolated from the bonded Terfenol-D composite. The ME voltage coefficients of these 10 sections were measured individually and in parallel/series modes. The ME voltage coefficient,  $\alpha_{E,31}$ , was measured in the ME measurement system. (The automatic testing software was supported by Jun Lu, State Key Laboratory of Magnetism, Institute of Physics, Chinese Academy of Sciences, Beijing 100190, China), in which the DC bias and AC magnetic fields were applied along the length of the sample. The output voltage,  $\delta V$ , across the sample was measured by an oscilloscope. The ME voltage coefficient was calculated as:  $\alpha_{E,31} = \delta V / (t_{\text{PZT}} \delta H)$ , where  $t_{\text{PZT}}$  is the PZT thickness,  $\delta H$  is the amplitude of the AC magnetic field generated by the Helmholtz coils. In the experiment, the AC current flowing through the coil with the amplitude of  $\delta H = 1.2 \text{ Oe}$  is equal to 1 A.<sup>18,30,31</sup> The signal-to-noise ratio in our measurement was larger than 20 dB.

The frequency dependence of  $\alpha_{E,31}$  for the individual sections was measured under the DC magnetic field of  $H_{\text{DC}} = 380 \text{ Oe}$ , as shown in Fig. 2. There are two groups according to the  $\alpha_{E,31}$  value. The central sections (3<sup>rd</sup> and 8<sup>th</sup>) and the sub-central sections (2<sup>nd</sup>, 4<sup>th</sup>, 7<sup>th</sup> and 9<sup>th</sup>) exhibit much larger magnetolectric coefficients, more than twice higher than the marginal sections (1<sup>st</sup>, 5<sup>th</sup>, 6<sup>th</sup> and 10<sup>th</sup>). This dissimilarity could be caused by different stresses applied to the different parts of the PZT plate. The bonded Terfenol-D composite vibrates along the length direction under the AC magnetic field. This longitudinal vibration transforms into bending vibration when one PZT plate is glued to the Terfenol-D composite due to the difference of Young's modulus between the PZT and bonded Terfenol-D composite.<sup>32</sup> Nan *et al.*, performed the vibration modal analysis by using a laser Doppler vibrometer.<sup>33</sup> The out-of-plane vibration displacement measurement result showed that the central area exhibits largest distortion. Due to the large deflection and the slope in the central and sub-central areas of the bonded Terfenol-D composite, indicated by the circles in Fig. 2, larger stresses are applied to the 3<sup>rd</sup>, 8<sup>th</sup>, 2<sup>nd</sup>, 4<sup>th</sup>, 7<sup>th</sup> and 9<sup>th</sup> sections of the PZT plate, resulting in different magnetolectric coefficients between the 10 sections.

The ME coefficient of sections 3 and 8 are 9.08 and 9.32 V/cm·Oe, respectively. The ME coefficient of these two sections connected in series,  $\alpha_{3+8}$ , should be about 18 V/cm·Oe, if they were two separate parts, according to the previous study.<sup>18</sup> However, the results showed that the  $\alpha_{3+8}$  is 14.97 V/cm·Oe. It can be concluded that the “missing ME effect” is caused by the middle

FIG. 2. The frequency dependence of  $\alpha_{E,31}$  with  $H_{DC}=380$  Oe.

part between sections 3 and 8. In the series mode, the positive electrode of section 3 (3+) and the negative electrode of section 8 (8-) are connected to the measurement system, and 3- and 8+ are connected with a conducting wire. To gain a better understanding of the effect of the middle part, 3- and 8+ were disconnected when measuring the ME coefficient of the sections 3 and 8 connected in series, as shown in Fig. 3. In this case, it can be treated as a capacitor with nearly zero overlap area. The  $\alpha_{3+8,dis}$  is 4.93 V/cm·Oe, which can be regarded as the “missing ME effect” caused by the middle part and edge areas of the sections 3 and 8. The “missing ME effect” is shielded when the sections 3- and 8+ were connected, because the middle part and edge areas of the sections 3 and 8 were short-circuited. The results show that every two serial sections exhibit the same rule.

The  $\alpha_{P1-10}$  is 10.15 V/cm·Oe when the 10 sections were connected in parallel, which is equal to that of an intact PZT plate. This electrode-arrayed ME composite is expected to display an enhanced ME coefficient when the 10 sections are connected in series. However, the  $\alpha_{S1-10}$  is only 12.82 V/cm·Oe when the 10 section were connected in series in the numerical order. Fig. 4 shows the serial ME coefficient with the number of sections increasing from 1 to 10. It can be seen that the ME coefficient is decreased when the sub-central sections (2<sup>nd</sup>, 4<sup>th</sup>, 7<sup>th</sup> and 9<sup>th</sup>) are connected into a sequence. Other connecting sequences share the same rule, such as 1+2+3+4+5+10+9+8+7+6, 1+10+9+2+3+8+7+4+5+6, 1+6+10+5+9+4+2+7+3+8, etc. This may be due to the mismatch of the amount of charge between the different sections. The sections with less amount of charge decrease the serial ME coefficient.

To solve this mismatch, sections with less amount of charge were first connected in parallel and then serially connected with the sections with more charge. Fig. 5 shows the optimized connecting sequence. Sections 3 and 8, which possess almost the same amount of charge, were serially connected. Sections 2 and 9 were connected in parallel and then serially connected with section 3. Sections 1, 5, 6, 10, which possess the least amount of charge, were connected in parallel to match sections 3 and 8. The ME coefficient of this connecting sequence  $\alpha_{optimized}$  is 19.25 V/cm·Oe, which is almost double that of the un-arrayed condition.

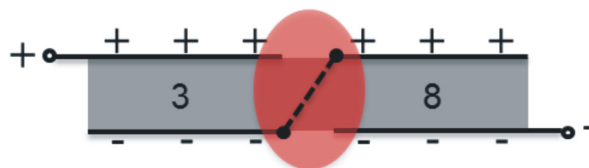


FIG. 3. Schematics of the sections 3 and 8 connected in series.

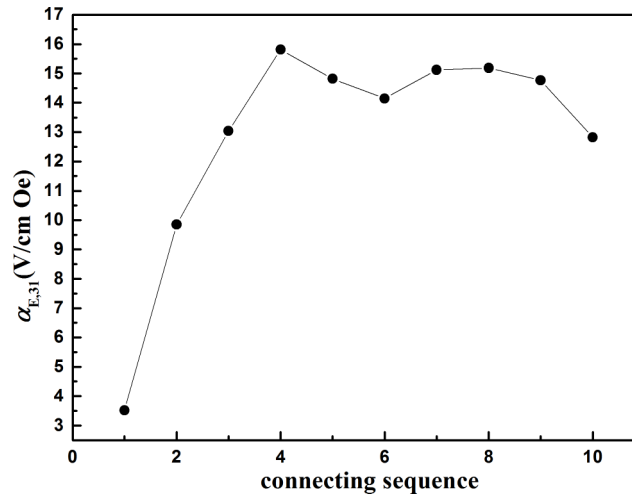


FIG. 4. The ME coefficient of the serial mode in the numerical order.

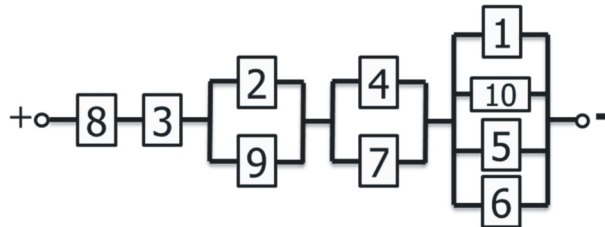


FIG. 5. Optimized connecting sequence.

In conclusion, the central and sub-central sections exhibit much larger magnetoelectric coefficients than marginal sections due to the different stress state under resonance. The magnetoelectric coefficient is doubled compared with the un-arrayed condition when the 10 sections are parallel/serially connected in an optimized connecting sequence. Based on these results, optimized array patterns can be designed according to the specific composite requirements to obtain additional magnetoelectric effect from the original composite structure. This electrode-arrayed configuration can also be applied to other ME composite structures to increase their ME effect, and be used as the analysis method to better understand the ME effect in different areas of laminate composites.

## ACKNOWLEDGMENTS

This work was supported by the Beijing Nova program (Z141103001814006), by the National Key Technology R&D Program (No. 2012BAC12B05 and 2012BAC02B01), by the National Natural Science Foundation of China (No. 51174247 and U1360202), by the National High-Tech Research and the Development Program of China (No. 2012AA063202).

- <sup>1</sup> H. Schmid, *Ferroelectrics* **162**, 317 (1994).
- <sup>2</sup> M. Fiebig, *J. Phys. D* **38**, R123 (2005).
- <sup>3</sup> V. J. Folen, G. T. Rado, and E. W. Stalder, *Phys. Rev. Lett.* **6**, 607 (1961).
- <sup>4</sup> S. D. Kaushik, S. Rayaprol, J. Saha, N. Mohapatra, V. Siruguri, P. D. Babu, S. Patnaik, and E. V. Sampathkumaran, *J. Appl. Phys.* **108**, 084106 (2010).
- <sup>5</sup> J. Magesh, P. Murugavel, R. V. K. Mangalam, K. Singh, Ch. Simon, and W. Prellier, *J. Appl. Phys.* **112**, 104116 (2012).
- <sup>6</sup> G. Srinivasan, I. V. Zavislyak, and A. S. Tatarenko, *Appl. Phys. Lett.* **89**, 152508 (2006).
- <sup>7</sup> J. Zhai, S. Dong, Z. Xing, J. Li, and D. Vieland, *Appl. Phys. Lett.* **91**, 123513 (2007).
- <sup>8</sup> H. Greve, E. Woltermann, R. Jahns, S. Marauska, B. Wagner, R. Knöchel, M. Wuttig, and E. Quandt, *Appl. Phys. Lett.* **97**, 152503 (2010).
- <sup>9</sup> T. Wu and G. P. Carman, *J. Appl. Phys.* **112**, 073915 (2012).
- <sup>10</sup> Y. Zhou, D. J. Apo, and S. Priya, *Appl. Phys. Lett.* **103**, 192909 (2013).

- <sup>11</sup> J. T. Zhang, P. Li, Y. M. Wen, W. He, A. C. Yang, C. J. Lu, J. Qiu, J. Wen, J. Yang, Y. Zhu, and M. Yu, *Rev. Sci. Instrum.* **83**, 115001 (2012).
- <sup>12</sup> J. G. Wan, X. W. Wang, Y. J. Wu, M. Zeng, Y. Wang, H. Jiang, W. Q. Zhou, G. H. Wang, and J.-M. Liu, *Appl. Phys. Lett.* **86**, 122501 (2005).
- <sup>13</sup> K. Bi and Y. G. Wang, *Solid State Commun.* **150**, 248 (2010).
- <sup>14</sup> N. Cai, J. Y. Zhai, L. Liu, Y. H. Lin, and C. W. Nan, *Mater. Sci. Eng., B* **99**, 211 (2003).
- <sup>15</sup> J. P. Zhou, S. Zhang, G. Liu, H. C. He, and C. W. Nan, *Acta. Phys. Sin.* **55**, 3766 (2006).
- <sup>16</sup> C. W. Nan, *Phys. Rev. B* **50**, 6082 (1994).
- <sup>17</sup> J. Q. Gao, D. Hasanya, Y. Shen, Y. J. Wang, J. F. Li, and D. Viehland, *J. Appl. Phys.* **112**, 104101 (2012).
- <sup>18</sup> Z. J. Zuo, D. A. Pan, J. Lu, S. G. Zhang, J. J. Tian, L. J. Qiao, and A. A. Volinsky, *Appl. Phys. Lett.* **104**, 032906 (2014).
- <sup>19</sup> G. J. Wu, R. Zhang, X. Li, and N. Zhang, *J. Appl. Phys.* **110**, 124103 (2011).
- <sup>20</sup> G. X. Liu, X. X. Cui, and S. X. Dong, *J. Appl. Phys.* **108**, 094106 (2010).
- <sup>21</sup> S. C. Yang, C. S. Park, K. H. Cho, and S. Priya, *J. Appl. Phys.* **108**, 093706 (2010).
- <sup>22</sup> H. C. Liu, C. G. Quan, C. J. Tay, T. Kobayashi, and C. Lee, *Phys. Procedia* **19**, 129 (2011).
- <sup>23</sup> J. Rajagopalan, K. Balasubramaniam, and C. V. Krishnamurthy, *Smart Mater. Struct.* **15**, 1190 (2006).
- <sup>24</sup> J. S. Park, S. H. Lee, S. S. Park, J. W. Cho, S. W. Jung, J. H. Han, and S. G. Kang, *Sens. Actuators, A* **108**, 206 (2003).
- <sup>25</sup> V. Ferrari, D. Marioli, A. Taroni, and E. Ranucci, *Sens. Actuators, B* **68**, 81 (2000).
- <sup>26</sup> Z. Shi, C. W. Nan, J. Zhang, N. Cai, and J.-F. Li, *Appl. Phys. Lett.* **87**, 012503 (2005).
- <sup>27</sup> S. X. Dong, J. Y. Zhai, F. M. Bai, J. F. Li, and D. Viehland, *Appl. Phys. Lett.* **87**, 062502 (2005).
- <sup>28</sup> S. X. Dong, J. Y. Zhai, J. F. Li, and D. Viehland, *Appl. Phys. Lett.* **89**, 252904 (2006).
- <sup>29</sup> Z. P. Xing, J. Y. Zhai, J. F. Li, and D. Viehland, *J. Appl. Phys.* **106**, 024512 (2009).
- <sup>30</sup> Z. J. Zuo, D. A. Pan, Y. M. Jia, J. J. Tian, S. G. Zhang, and L. J. Qiao, *J. Alloys Compd.* **587**, 287 (2014).
- <sup>31</sup> Z. J. Zuo, D. A. Pan, Y. M. Jia, S. G. Zhang, and L. J. Qiao, *AIP Adv.* **3**, 122114 (2013).
- <sup>32</sup> N. Zhang, D. K. Liang, T. Schneider, and G. Srinivasan, *J. Appl. Phys.* **101**, 083902 (2007).
- <sup>33</sup> Z. Shi, J. Ma, and C. W. Nan, *J. Electroceram.* **21**, 390 (2008).